

# Wrinkling hierarchy in constrained thin sheets from suspended graphene to curtains

Hugues Vandeparre<sup>1,\*</sup>, Miguel Piñeirua<sup>2,\*</sup>, Fabian Brau<sup>1</sup>, Benoit Roman<sup>2</sup>, José Bico<sup>2</sup>,  
Cyprien Gay<sup>3</sup>, Wenzhong Bao<sup>4</sup>, Chun Ning Lau<sup>4</sup>, Pedro M. Reis<sup>5</sup>, Pascal Damman<sup>1</sup>

<sup>1</sup>Laboratoire Interfaces & Fluides Complexes, CIRMAP,

Université de Mons, 20 Place du Parc, B-7000 Mons, Belgium

<sup>2</sup>PMMH, CNRS UMR 7636, ESPCI, ParisTech, Univ. Paris 6 & Paris 7,  
10 Rue Vauquelin, 75231 Paris Cedex 05, France

<sup>3</sup>Matière et Systèmes Complexes, Université Paris Diderot - Paris 7,  
CNRS, UMR 7057, Bâtiment Condorcet, F-75205 Paris cedex 13, France

<sup>4</sup>Department of Physics and Astronomy, University of California, Riverside, California 92521, USA and

<sup>5</sup>Departments of Mechanical Engineering and Civil & Environmental Engineering,  
Massachusetts Institute of Technology, Cambridge, Massachusetts 02139, USA

(Dated: May 10, 2022)

**The drive towards miniaturization in technology is demanding for increasingly thinner components, raising new mechanical challenges [1]. Thin films are however unstable to boundary or substrate-induced compressive loads. Moderate compression results in regular wrinkling [2–9] while further confinement can lead to crumpling [10–12]. Regions of stress focusing can be a hindrance, acting as nucleation points for mechanical failure. Conversely, they can be exploited constructively for tunable thin structures. For example, singular points of deformation dramatically affect the electronic properties of graphene [13]. Here, we show that thin sheets under boundary confinement spontaneously generate a universal self-similar hierarchy of wrinkles; from strained suspended graphene to ordinary hanging curtains. We develop a formalism based on *wrinklons*, a localized transition zone in the merging of two wrinkles, as building-blocks to describe these wrinkled patterns. Our approach may find applications in domains such as graphene-based electronics [14], fuel cell technology [15], thin-film solar cells [16] or draping in virtual reality [17, 18].**

Figure 1 shows some recent technological systems composed of wrinkled graphene sheets (Fig. 1a) and fuel cell membranes (Fig. 1b), along with an ordinary hanged curtain (Fig. 1c). The diversity and complexity of those systems, characterized by various chemical and physical conditions, could suggest, *a priori*, that the underlying mechanisms governing the formation of these patterns are unrelated. However, those systems can be depicted, independently from the details of the experiments, as a thin sheet constrained at one edge while the others are free to adapt their morphology. These constraints can take the form of an imposed wavelength at one edge or just the requirement that it should remain flat. As illustrated in Fig. 1 and 2, sheets made from various materials constrained at one edge by an imposed sinusoidal profile (amplitude,  $A_0$  and wavelength,  $\lambda_0$ ) spontaneously develop a hierarchical pattern of folds or wrinkles similar to those

observed for technologically relevant thin films. At first sight, these patterns consist of a hierarchy of successive generations of folds whose typical size gradually increases along  $x$ , as illustrated in Fig. 1c. These hierarchical patterns can be rationalized by considering the variation of the average wavelength,  $\lambda$ , with the distance to the constrained edge,  $x$ . This evolution is adequately described by a simple power law,  $\lambda \sim x^m$ , which suggests that the morphology is self-similar, see Fig. 1d. The exponent,  $m$ , is a robust feature of these folding patterns: curtains made of various materials with contrasted properties possess similar exponents, close to  $2/3$  for light sheets or  $1/2$  for heavy sheets.

Assuming inextensibility of the sheet along the  $y$  direction, the imposed undulation along this direction exactly compensates for an effective lateral compression of the membrane by a factor  $(1 - \Delta)$  defined as,

$$(1 - \Delta) \equiv W/W_0 = W / \int_0^W \sqrt{1 + (\partial z / \partial y)^2} dy, \quad (1)$$

where  $W_0$  and  $W$  are the curvilinear and projected width of the curtain, respectively, and  $z(x, y)$  is the out-of-plane deformation of the sheet. At any position along the  $x$  axis, the function  $z(x, y)$  is typically sinusoidal along  $y$ , with an amplitude  $A(x)$  and a wavelength  $\lambda(x)$ . According to equation (1), these quantities are related by  $\Delta \sim (A(x)/\lambda(x))^2$  at the lowest order, where the lateral compression  $\Delta$  is assumed to be constant throughout the length of the curtain. The undulations of the sheet along  $y$  are characterized by a curvature  $\kappa \simeq \partial^2 z / \partial y^2$  whose typical value, varying along  $x$ , is of order  $\kappa(x) \sim A/\lambda^2$ . The corresponding energy per unit area,  $u_b$ , for bending the membrane is thus of order  $u_b \sim Eh^3 \kappa^2 \sim Eh^3 \Delta/\lambda^2$ , where  $E$  is the Young modulus and  $h$  the thickness of the sheet. Since  $u_b$  is proportional to  $1/\lambda^2$ , the membrane adopts the largest possible wavelengths, in order to minimize energy. This tendency to increase the wavelength, combined with the constraint imposed at the boundaries, constitutes the underlying mechanism of the observed hierarchical wrinkling pattern.

The allometric laws mentioned above can be derived by considering that the global pattern results from the self-assembly of building-blocks which we denote *wrinklons*. A single wrinklon corresponds to the localized transition zone needed for merging two wrinkles of wavelength  $\lambda$  into

\*These authors contributed equally to this work

a larger one of width  $2\lambda$ . This wavelength transition requires a distortion of the membrane which is relaxed over a distance  $L$ . In other words, each wrinklon is characterized by a size,  $L$ , which, *a priori*, depends on the material properties and the wavelength  $\lambda$ . This length  $L$  can also be viewed as the persistence length of a specific generation of wrinkles. To investigate the properties and behavior of wrinklons, we have performed model experiments using thin plastic sheets with thicknesses ranging from 30 to 250  $\mu\text{m}$ . The sheets were constrained with sinusoidal clamps: two opposite edges are constrained by a wavelength  $\lambda$  (amplitude  $A$ ) and  $2\lambda$  (amplitude  $2A$ ), respectively, see Fig. 2a,b. The normalized length of the transition domain, that is the size of the wrinklons,  $L/\lambda$ , is plotted in Fig. 2c as a function of the normalized amplitude,  $A/h$ ; the data collapse on a single curve defined by  $L/\lambda \sim \sqrt{A/h}$ . This implies that  $L \sim \lambda^{3/2}$  since  $A \sim \lambda\sqrt{\Delta}$ .

These wrinklons can be assembled to mimic the behavior of a wrinkling cascade. Indeed, if  $L$  is the distance over which the wavelength increases from  $\lambda$  to  $2\lambda$ , its variation,  $d\lambda/dx$ , is thus of order  $\lambda/L$ . Hence, the evolution of  $\lambda$  as a function of the distance from the constrained edge,  $x$ , is given by

$$\frac{d\lambda}{dx} \simeq \frac{\lambda}{L}. \quad (2)$$

If  $L$  was independent of  $\lambda$ , then  $\lambda(x)$  would evolve exponentially. However, as discussed below, the balance between the energy terms describing a distorted membrane implies that  $L(\lambda)$  and  $\lambda(x)$  are instead both described by power-laws, according to equation (2). Considering the scaling  $L \sim \lambda^{3/2}$  deduced from the above single wrinklon experiments, equation (2) yields the evolution of the wavelength along the sheet,  $\lambda \sim x^{2/3}$ . The excellent agreement between this power law and the experimental data measured for light sheets (Fig. 1d) provides a strong support to the concept of wrinklons as building-blocks. Equation (2) can now be regarded as a tool that connects the properties of single wrinklons to the features of the full wrinkling-cascade pattern. Consequently, in order to rationalize the scaling law describing a hierarchy, one needs to derive a theoretical expression for  $L(\lambda)$  by studying the mechanics of these building-blocks in detail.

When a thin sheet is strongly confined, it generally crumples. Since stretching deformations are costly with respect to pure bending, the sheet tends to adopt an isometric (developable) shape [11]. However, in most cases, the only developable solution compatible with boundary conditions would include flat domains surrounded by edge or point-like singularities. These crumpling singularities which focus the elastic energy into narrow regions have been classified as developable cones [19, 20], ridges [10, 21], or curved ridges [22]. In our case, the scenario is however significantly different; in contrast to crumpling, we show that stretching is smoothly distributed in the transition zone. We illustrate this transition by considering the limiting case of vanishing thickness mimicked by origami (a tightly folded paper sheet). Figure 3a shows an origami model of the  $\lambda$  to  $2\lambda$  transition domain, which clearly

shows that the membrane has to be stretched to connect these periodic patterns and bridge the existing hole. Consequently, the sheet can no longer be isometrically deformed in the transition domain from an initially flat surface (even if singularities are included). This unusual geometric constraint leads to a non-crumpled solution, since the unavoidable stretching energy is minimized when it is distributed over the entire transition domain. This stretching energy can be estimated through the elongation strain of the sheet along  $x$  within a transition domain. Considering the slope of the sheet,  $\alpha \sim A/L \sim \lambda\Delta^{1/2}/L$  (Fig. 3b), the typical value of the strain along  $x$  is of order  $\alpha^2$ . The stretching energy thus reads

$$U_s \sim Eh(\alpha^2)^2 L\lambda \sim Eh\lambda^5\Delta^2L^{-3}.$$

As shown in Figs. 1 and 2, wrinklons should also include a tip singularity (a small region where Gaussian curvature is large). This singularity can be described as a semi-circular fold of radius  $\rho$  (Fig. 2b). The energy of these singularities has been derived by Pogorelov [22, p. 10] and more recently by Pauchard [23] in a study of deformed shells. In our context, the energy of such curved folds reads

$$U_{\text{cf}} \sim Eh^{5/2}\alpha^{5/2}\rho^{1/2} \sim Eh^{5/2}\Delta^{5/4}\lambda^{7/2}L^{-3},$$

where the radius at the tip of the wrinklon is taken as  $\rho \sim \lambda^2/L$ . This expression is suggested by the roughly parabolic shape of the crest of the defect in Fig. 2b. The validity of this geometric relationship is confirmed by the evolution of  $\rho$  shown in the inset of Fig. 2c. Nevertheless, the ratio of the curved fold energy to the stretching energy of the wrinklon,  $U_{\text{cf}}/U_s \sim (h/A)^{3/2}$ , is small in our experiments, not exceeding 0.03. The effect of this concentrated region can therefore be neglected in the following.

The total energy of a wrinklon, whose area scales as  $L\lambda$ , is thus given by  $U_{\text{tot}} = U_s + U_b \simeq Eh\lambda^5\Delta^2L^{-3} + Eh^3\Delta L\lambda^{-1}$ . The size of a single wrinklon is obtained by minimizing this total energy with respect to  $L$  yielding

$$L(\lambda) \sim \Delta^{1/4}\lambda^{3/2}h^{-1/2}. \quad (3)$$

Equation (3) is in close agreement with the experimental data reported in Fig. 2c. Indeed, considering that  $A \sim \lambda\sqrt{\Delta}$ , this equation can be rewritten as  $L \sim \lambda\sqrt{A/h}$ . The scaling for the wavelength describing the whole hierarchical pattern is obtained by integration of equation (2) with  $L(\lambda)$  given by equation (3) and is found to be

$$\frac{\lambda(x)\Delta^{1/6}}{h} \sim \left(\frac{x}{h}\right)^{2/3}. \quad (4)$$

This scaling,  $\lambda \sim x^{2/3}$ , is in very good agreement with the observed power laws for light curtains, *e.g.* made of fabric or paper sheets (Fig. 1d). In addition to yielding the proper exponent, this relation enables the comparison of the data obtained from seemingly disparate systems, over a wide range of lengthscales and independently of material properties. Figure 4a provides a remarkable collapse of the evolutions of the wavelengths measured with light curtains and various thin plastic sheets.

Heavy curtains, made from fabric or rubber, and constrained graphene bilayers do not follow this peculiar behaviour. Instead, we observe that  $\lambda \sim x^{1/2}$  (Fig. 1d). In these experiments, an additional tensile force is however acting on the sheet. This tension,  $T$ , is given by the longitudinal tensile strain induced by thermal manipulation in the case of graphene sheets (annealing temperature, 523 K) [8] and by the gravity for heavy curtains ( $T = \rho_c g h (H - x) \sim \rho_c g h H$ , where  $x$ ,  $\rho_c$ ,  $g$ ,  $h$ , and  $H$  are the distance from the constrained edge, the density of the curtain, the gravity constant, the thickness and the height of the curtain, respectively). These systems can be compared to the cascade of wrinkles observed for compressed thin polystyrene films on an air-water interface [24, 25]. The surface tension of water at the free edges provides an equivalent tensile force applying to the thin sheet.

The tension, that is a uniaxial tensile force exerted along  $x$  per unit width, imposes an additional stretching energy given by

$$U_t \sim T \alpha^2 L \lambda \sim T \Delta \lambda^3 L^{-1},$$

and becomes dominant when  $U_t > U_s$ , that is when  $T > E h^2 \Delta / A$ . The total energy of the distorted membrane thus becomes  $U_{\text{tot}} = U_t + U_b$ . The length of a wrinkle found from the minimization of  $U_{\text{tot}}$  is

$$L(\lambda) \sim \frac{\lambda^2}{h} \sqrt{\frac{T}{E h}}. \quad (5)$$

As expected, the tensile force thus increases the length of wrinkles for a given wavelength [26]. By integration, we obtain the corresponding spatial evolution of the wavelength along an heavy sheet

$$\frac{\lambda(x)}{h} \sim \left( \frac{E h}{T} \right)^{1/4} \left( \frac{x}{h} \right)^{1/2}. \quad (6)$$

This scaling is in excellent agreement with the power laws observed for heavy curtains and graphene bilayers,  $\lambda \sim x^{1/2}$  (Fig. 1d). By using equation (6), the data of various macroscopic curtains, graphene bilayers and nanometric polystyrene films [24] collapse onto a single master curve with no fitting parameters (see Fig. 4b). It is important to note that the wavelength data used to build this master curve span over 7 orders of magnitude. Our formalism is thus validated from hundreds of nm for graphene sheets to meters for rubber and fabric curtains, which points to the universality of our description.

In previously reported fractal buckling of torn plastic sheets [27], the imposed metric determines the three-dimensional shape of the distorted membrane, characterized by a superposition of various modes [28]. However, the patterns observed here for constrained thin sheets exhibit a continuous evolution of the wavelength. We also show that this natural tendency of a rigid membrane can be readily manipulated by applying an internal or external tension (see equation (6)). The magnitude of the tension is the control parameter that affects the pattern of folds via the size and energy cost of a single wrinkle. For example, for large values of tension, we would even expect a transition toward a purely cylindrical pattern with a single wavelength.

According to our theoretical description, the formation of hierarchical/self-similar patterns of wrinkles can be understood predictively. From a technological point of view, this knowledge opens the opportunity to avoid undesirable wrinkles or, more interestingly, to control wrinkles and create thin sheets with a gradient in their local topography. For instance, the ability of graphene to conduct electricity varies with the local shape of the membrane [8, 13, 14, 29]. A sheet exhibiting a hierarchy of wrinkles would then exhibit a continuous controlled variation of electronic properties. For metrological purposes, this study also demonstrates that strains in thin sheet can be easily estimated by visual inspection of self-similar wrinkling patterns.

## Methods

**Curtains.** The curtain experiments were carried out using fabric: thicknesses 220  $\mu\text{m}$ , density  $\rho_c = 820 \text{ kg/m}^3$  and elastic modulus  $E \sim 1 \text{ MPa}$ ; latex: thicknesses 220 and 400  $\mu\text{m}$ , density  $\rho_c = 980 \text{ kg/m}^3$  and elastic modulus  $E \sim 1 \text{ MPa}$ ; paper: thickness 125  $\mu\text{m}$ . The fabric curtain was 4 m long and 2.5 m wide, while for the rubber and paper curtains were 2 m long and 1 m wide. Each curtain was hung with an imposed sinusoidal boundary condition through an array of screws of tunable length. The wavelength was fixed to  $\lambda = 20 \text{ mm}$  with an amplitude  $A$  spanning from 1.2 to 8 mm. The bottom edges of the curtains were left free except for the ballasted curtain experiments where 10 steel disks of 180 g each were hung from the bottom edge with a spacing of 100 mm in between. The average wavelength was obtained by dividing the total width of the curtain by the number of wrinkles found at a given distance from the constrained edge.

**Graphene bilayers.** Suspended graphene membranes were prepared by standard mechanical cleavage technique on Si/SiO<sub>2</sub> wafers with pre-patterned trenches. Bilayer graphene sheets were identified by color contrast in an optical microscope and/or Raman spectroscopy [8]. The Si substrates were p-doped, and the thickness of silicon and SiO<sub>2</sub> are 0.5 mm and 300 nm, respectively. The trenches, fabricated at the UCSB Nanofabrication facility, were defined by photolithography followed by plasma etching in a reactive ion etcher (RIE) system. Strain in graphene sheets was estimated using the same procedure as the one used to produce Fig. 1e in Ref. [8].

**Isolated wrinkles.** These experiments were carried out using A4 size sheets made of biaxially oriented polypropylene (BOPP Innovia) of thicknesses 30, 50, 90, 100 and 250  $\mu\text{m}$  and elastic modulus  $E \sim 2.6 \text{ GPa}$ . To impose a sinusoidal condition at the edge of the sheet we used Plexiglas clamps of thickness 5 mm with sinusoidal profiles of different amplitudes and wavelengths to clamp the sheets: fixed amplitude  $A = 3 \text{ mm}$  with wavelengths  $\lambda = 13, 18, 26$  and 58 mm; fixed wavelength  $\lambda = 24 \text{ mm}$  with amplitudes  $A = 3, 4, 5, 6$  and 7 mm. A second clamp of wavelength  $2\lambda$  and amplitude  $2A$  was used to impose a second profile condition for the sheet at a certain distance  $L_2$  away from the clamped edge. In this way we forced the sheet to switch from the initial wavelength  $\lambda$  to the next wavelength  $2\lambda$ , thus generating the formation of a controlled wrinkle. The distance  $L_2$  was selected by separating progressively the opposite clamps until the shape of the wrinkles became stationary.

- 
- [1] Rogers, J. A. & Huang, Y. A curvy, stretchy future for electronics. *Proc. Nat. Acad. Sci.* **106**, 10875-10876 (2009).
- [2] Milner, S.T., Joanny, J.F. & Pincus P. Buckling of Langmuir Monolayers. *Europhys. Lett.* **9**, 495-500 (1989).
- [3] Bowden, N., Brittain, S., Evans, A. G., Hutchinson, J. W. & G. M. Whitesides. Spontaneous formation of ordered structures in thin films of metals supported on an elastomeric polymer. *Nature* **393**, 146-149 (1998).
- [4] Cerda, E., Ravi-Chandar, K. & Mahadevan, L. Wrinkling of an elastic sheet under tension. *Nature* **419**, 579-580 (2002).
- [5] Cerda, E. & Mahadevan, L. Geometry and physics of wrinkling. *Phys. Rev. Lett.* **90**, 074302 (2003).
- [6] Huang, J. *et al.* Capillary Wrinkling of Floating Thin Polymer Films. *Science* **317**, 650-653 (2007).
- [7] Pocivavsek, L. *et al.* Stress and fold localization in thin elastic membranes. *Science* **320**, 912-916 (2008).
- [8] Bao, W., Miao, F., Chen, Z., Zhang, H., Jang, W., Dames, C. & Lau, C. N. Controlled ripple texturing of suspended graphene and ultrathin graphite membranes. *Nature Nanotech.* **4**, 562-566 (2009).
- [9] Brau, F., Vandeparre, H., Sabbah, A., Poulard, C., Boudaoud, A. & Damman, P. Multiple-length-scale elastic instability mimics parametric resonance of nonlinear oscillators. *Nature Phys.* in press.
- [10] Lobkovsky, A., Gentges, S., Li, H., Morse, D. & Witten, T. A. Scaling Properties of Stretching Ridges in a Crumpled Elastic Sheet. *Science* **270**, 1482-1485 (1995).
- [11] Witten, T. A. Stress focusing in elastic sheets. *Rev. Mod. Phys.* **79**, 643-675 (2007).
- [12] Audoly, B. & Pomeau, Y. *Elasticity and geometry: from hair curls to the nonlinear response of shells* (Oxford University Press, Oxford, 2010).
- [13] Pereira, V. M., Castro Neto, A. H., Liang, H. Y. & Mahadevan, L. Geometry, Mechanics, and Electronics of Singular Structures and Wrinkles in Graphene. *Phys. Rev. Lett.* **105**, 156603 (2010).
- [14] Novoselov, K. S. *et al.* Electric Field Effect in Atomically Thin Carbon Films. *Science* **306**, 666-669 (2004).
- [15] Lai, B.-K., Kerman, K. & Ramanathan, S. On the role of ultra-thin oxide cathode synthesis on the functionality of micro-solid oxide fuel cells: Structure, stress engineering and in situ observation of fuel cell membranes during operation. *J. Power Sources* **195**, 5185-5196 (2010).
- [16] Ludwig, C. D. R., Gruhn, T., Felser, C., Schilling, T., Windeln, J. & Kratzer, P. Indium-Gallium Segregation in  $\text{CuIn}_x\text{Ga}_{1-x}\text{Se}_2$ : An Ab Initio-Based Monte Carlo Study. *Phys. Rev. Lett.* **105**, 025702 (2010).
- [17] Cerda, E., Mahadevan, L. & Pasini, J. M. The element of draping. *Proc. Nat. Acad. Sci.* **101**, 1806-1810 (2004).
- [18] Wang, Y., Wang, C. C. L. & Yuen, M. M. F. Fast energy-based surface wrinkle modeling. *Comput. Graph.-UK* **30**, 111-125 (2006).
- [19] Ben Amar, M., & Pomeau, Y. Crumpled paper. *Proc. R. Soc. Lond. A* **453**, 729-755 (1997).
- [20] Cerda, E., Chaieb, S., Melo, F. & Mahadevan, L. Conical dislocations in crumpling. *Nature* **401**, 46-49 (1999).
- [21] Pomeau, Y. & Rica, S. Plaques très comprimées. *C. R. Acad. Sci. Paris* **325**, 181-187 (1997).
- [22] Pogorelov, A. V. *Bendings of surfaces and stability of shells*, Translations of Mathematical Monographs **72** (American Mathematical Society, Providence, RI, 1988).
- [23] Pauchard, L., Pomeau, Y. & Rica, S. Élasticité des coques. *C. R. Acad. Sci. Paris* **324**, Série IIb, 1-8 (1997).
- [24] Huang, J., Davidovitch, B., Santangelo, C. D., Russell, T. P. & Menon, N. Smooth Cascade of Wrinkles at the Edge of a Floating Elastic Film. *Phys. Rev. Lett.* **105**, 038302 (2010).
- [25] Davidovitch, B. Period fissioning and other instabilities of stressed elastic membranes. *Phys. Rev. E* **80**, 025202(R) (2009).
- [26] Notice that, in principle, this length could also be obtained from a numerical analysis of the Euler-Lagrange equation for constrained thin sheets (B. Davidovitch, private communication).
- [27] Sharon, E., Roman, B., Marder, M., Shin, G. S. & Swinney, H. L. Buckling cascades in free sheets. *Nature* **419**, 579 (2002).
- [28] Audoly, B. & Boudaoud, A. Self-Similar Structures near Boundaries in Strained Systems. *Phys. Rev. Lett.* **91**, 086105 (2003).
- [29] de Juan, F., Cortijo, A. & Vozmediano, M. A. H. Charge inhomogeneities due to smooth ripples in graphene sheets. *Phys. Rev. B* **76**, 165409 (2007).

#### Acknowledgements

The authors thank B. Davidovitch, N. Menon, T. Witten for fruitful discussions. This work was partially supported by the Belgian National Funds for Scientific Research, the Government of the Region of Wallonia (REMANOS Research Programs), the European Science Foundation (Eurocores FANAS program, EBIOADI collaborative research project) and the French ANR Jeunes Chercheurs MecaWet and the MIT-France MISTI program. C.N.L. and W.B. acknowledge the support by ONR N00014-09-1-0724 and the FENA Focus Center. The theoretical part of this work was mostly completed at the Aspen Center for Physics.

#### Additional information

The authors declare no competing financial interests. Reprints and permissions information is available online at <http://npg.nature.com/reprintsandpermissions>. Correspondence and requests for materials should be addressed to P.D. ([pascal.damman@umons.ac.be](mailto:pascal.damman@umons.ac.be)).

#### Author contributions

P.D., P.M.R., B.R., J.B., H.V. and M.P. designed experiments on curtains and plastic sheets. C.N.L. and W.B. designed experiments on graphene sheets. M.P., H.V. and W.B. carried out experiments. M.P., H.V. and F.B. analyzed the data. F.B., P.D., C.G., B.R. and J.B. developed the theoretical model. P.D., F.B., B.R., P.M.R. and C.G. wrote the manuscript.

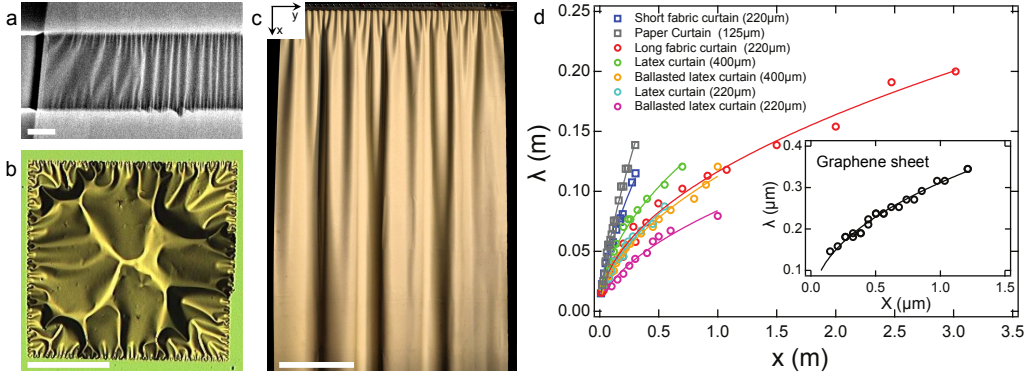


FIG. 1: **Morphology of constrained sheets.** **a**, SEM image of a graphene bilayer thin sheet suspended across pre-defined trenches on Si/SiO<sub>2</sub> substrates (the sample was annealed at 523K and tilted by 75° to improve the contrast in amplitude in SEM measurements). The scale bar is 1  $\mu$ m. **b**, Buckling of a La<sub>0.6</sub>Sr<sub>0.4</sub>Co<sub>0.8</sub>Fe<sub>0.2</sub>O<sub>3</sub> membrane released from SiN thin films using reactive ion etching and used in fuel cell technology [15], courtesy of Shriram Ramanathan. The scale bar is 0.1 mm. **c**, Hierarchical pattern of folds obtained for a long suspended curtain made of a thin sheet of rubber. The scale bar is 25 cm. **d**, Evolution of the average wavelength,  $\lambda$ , with the distance from the constrained edge,  $x$ , for various curtains as indicated. Power law fits are added (the power exponents are  $0.62 \pm 0.02$ , short fabric curtain;  $0.66 \pm 0.07$ , paper curtain;  $0.50 \pm 0.01$ , long fabric curtain;  $0.51 \pm 0.02$ , 400  $\mu$ m rubber curtain;  $0.53 \pm 0.03$ , 220  $\mu$ m rubber curtain;  $0.54 \pm 0.04$ , ballasted 220  $\mu$ m rubber curtain;  $0.53 \pm 0.02$ , ballasted 400  $\mu$ m rubber curtain). Inset: Evolution of  $\lambda$  with the distance from the constrained edge for the suspended graphene bilayer sheet shown in Fig. 1a (the power exponent is  $0.45 \pm 0.02$ ).

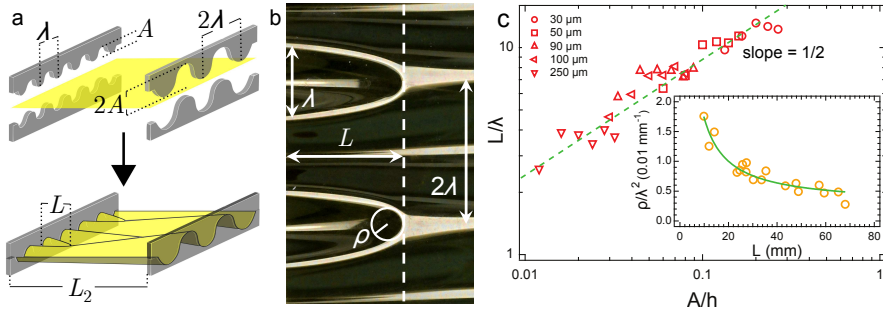


FIG. 2: **Properties of a single wrinklon.** **a**, Schematic representation of the single building-block experiments.  $L_2$  is defined in the Methods section. **b**, Morphology of the transition domain  $\lambda$  to  $2\lambda$  for a constrained plastic sheet for  $A = 6$  mm and  $\lambda = 8$  mm. **c**, Evolution of the normalized length of a wrinklon,  $L/\lambda$ , with the normalized amplitude,  $A/h$  for thin plastic sheets constrained with sinusoidal clamps (fixed wavelength,  $\lambda = 8$  mm). The thicknesses of the sheets vary from 30 to 250  $\mu$ m, as indicated. The inset shows the evolution of the normalized radius of curvature at the tip of the transition domain,  $\rho/\lambda^2$ , as a function of the length  $L$ . The solid line corresponds to a curve  $\rho/\lambda^2 \propto L^{-1}$ .

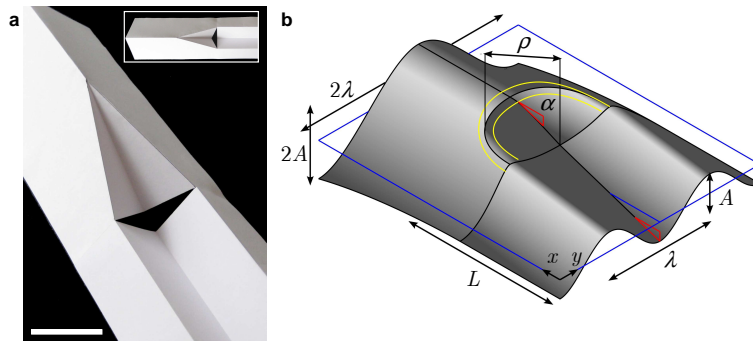


FIG. 3: **Morphology of wrinklons.** **a**, Origami describing the distorted domain at the  $\lambda$  to  $2\lambda$  transition. This toy model is illustrative of a sheet with a vanishing thickness and shows the necessity to stretch the sheet to connect both  $\lambda$  and  $2\lambda$  patterns. The scale bar is 5 cm. **b**, Schematic representation of the transition domain for sheets with finite thickness.

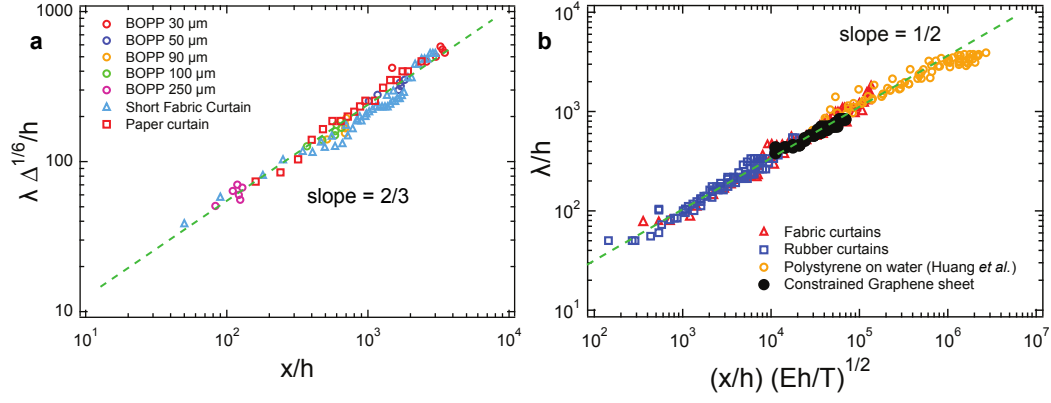


FIG. 4: **Master curves gathering all data.** **a**, Normalized wavelength,  $\tilde{\lambda}$ , as a function of the normalized distance,  $\tilde{x}$ , from the constrained edge for short light sheets (fabric curtain, paper curtain and constrained plastic sheets shown in Fig. 2). We use equation (4) for the normalization of the experimental data. The dashed line corresponds to the relation :  $\tilde{\lambda} = 2.89 \tilde{x}^{0.65}$ . **b**, Normalized wavelength as a function of the normalized distance from the constrained edge for sheets under tension: fabric curtains, rubber curtains, suspended bilayer graphene sheet and polystyrene thin films deposited on water from Ref. [24]. We use equation (6) for the normalization of the data. The dashed line corresponds to the relation :  $\tilde{\lambda} = 2.85 \tilde{x}^{0.52}$ .